Probing Structural Determinants Distal to the Site of Hydrolysis that Control Substrate Specificity of the 20S Proteasome

Michael Groll,[1,3] Tamim Nazif,[2] Robert Huber,[1] and Matthew Bogyo[2,3]
[1]Max Planck Institut für Biochemie
D-82152 Martinsried
Germany
[2]Department of Biochemistry and Biophysics
University of California, San Francisco
San Francisco, California 94143

Summary

The 20S proteasome is a large multicomponent protease complex. Relatively little is known about the mechanisms that control substrate specificity of its multiple active sites. We present here the crystal structure at 2.95 Å resolution of a $\beta2$-selective inhibitor (MB1) bound to the yeast 20S proteasome core particle (CP). This structure is compared to the structure of the CP bound to a general inhibitor (MB2) that covalently modified all three ($\beta1$, $\beta2$, $\beta5$) catalytic subunits. These two inhibitors differ only in their P3 and P4 residues, thereby highlighting binding interactions distal to the active site threonine that control absolute substrate specificity of the complex. Comparisons of the CP-bound structures of MB1, MB2, and the natural products epoxomycin and TMC-95A also provide information regarding general binding modes for several classes of proteasome inhibitors.

Introduction

The eukaryotic proteasome is a multicomponent proteolytic machine that contains multiple active sites within a central 20S core particle (CP). Further complexity results from the exchange of catalytic components upon γ-interferon stimulation, as well as the multitude of accessory proteins that can modulate the activity of the CP [1]. Regardless of these complexities of function, the structure and catalytic mechanism of the core particle of the proteasome have been firmly established [2–4].

The 20S proteasome is a large barrel-shaped protein complex composed of four rings of tightly packed subunits stacked upon one another. These rings of the 20S core particle are made up of proteins that can be classified into α and β subfamilies. The α subunits, constituting the top and bottom of the four ring stack, have substrate gating functions, while the β subunits supply the catalytic machinery found within the two central rings of the complex. In eukaryotes there are seven unique α and seven unique β subunits, each present in duplicate within a single CP. Of these seven β subunits ($\beta1$–$\beta7$), only three ($\beta1$, $\beta2$, $\beta5$) possess a catalytic N-terminal threonine residue required for hydrolysis of a protein substrate. Hydrolysis is initiated by attack of an amide bond by the hydroxyl nucleophile on the catalytic threonine (Figure 1A).

Since its discovery as a multicatalytic protease activity, the primary hydrolytic activities of the proteasome have been defined based on the identity of the amino acid found directly adjacent to the site of peptide bond hydrolysis [5–7]. These primary activities were initially defined by hydrolysis of fluorogenic peptide substrates and are termed the chymotrypsin-like (cleavage after hydrophobic residues), trypsin-like (cleavage after basic residues), and post glutamyl peptide hydrolyzing (PGPH) or caspase-like (cleavage after acidic residues) activities [8]. Studies of mutant enzymes in yeast as well as studies utilizing specific inhibitors in mammalian cells have helped to establish the roles of individual catalytic subunits in generating each of the primary hydrolysis activities [9–14]. These studies have linked the $\beta1$ subunit to the PGPH activity, the $\beta2$ subunit to the trypsin-like activity, and the $\beta5$ subunit to the chymotrypsin-like activity.

Recently, several studies using peptide-based inhibitors and peptide substrates have demonstrated an important role for amino acid residues distal to the site of hydrolysis [12, 13, 15–19]. In particular, the P3 and P4 positions play an important role in determining substrate binding to each of the active sites in the complex. These results indicate the importance of non-P1 interactions responsible for defining the absolute substrate specificity of the multiple active sites of the proteasome.

We present here the crystal structures of two peptide vinyl sulfones covalently bound to the yeast 20S proteasome complex. We have selected two compounds that differ in structure only in their P3 and P4 amino acid residues but that differ dramatically with respect to their subunit selectivity. The first inhibitor, MB1, binds only to the $\beta2$ active site while the other, MB2, binds to all three catalytic subunits ($\beta1$, $\beta2$, $\beta5$). The structures of these inhibitors provide insight into the global patterns of subunit specificity identified previously through library screening. Furthermore, overlay of the structure of MB1 bound into the active site of $\beta2$ with that of the nonsubunit selective, reversible inhibitor TMC-95A indicates a possible mechanism by which subunit-selective noncovalent inhibitors can be designed.

Results and Discussion

A number of elegant techniques have been developed to define global rules of primary substrate specificity of proteases [20–23]. These methods make use of libraries of peptide substrates that allow optimal sequences to be selected for a given purified enzyme. These sequences then provide information regarding the primary sequence specificity of the enzyme. However, such methods cannot be used for analysis of multicatalytic enzymes such as the proteasome due to the inability of the assay to resolve hydrolysis at multiple locations within a single enzyme complex. To circumvent these problems,

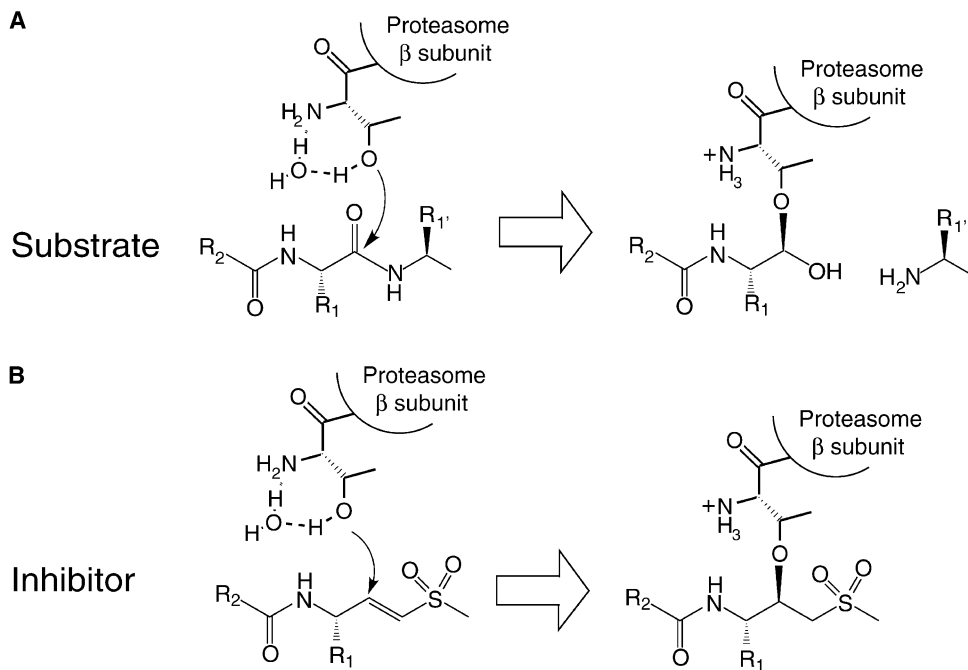[3]Correspondence: mbogyo@biochem.ucsf.edu (M.B.), groll@biochem.mpg.de (M.G.)

A

B

Figure 1. Catalytic Mechanism of the 20S Proteasome

(A) Peptide bond hydrolysis by the N-terminal threonine residue of a catalytic β subunit within the proteasome 20S core particle.
(B) Mechanism of covalent inhibition of the proteasome by Michael attack of a vinyl sulfone by the catalytic hydroxyl nucleophile of a proteasomal β subunit.

our laboratory previously developed libraries of peptide-based covalent inhibitors of the proteasome [12]. These inhibitors bind in a manner analogous to a bona fide protein substrate but are covalently locked into place by a nucleophilic attack on the inhibitory "warhead" (Figure 2B). Using this approach, it is possible to indirectly determine the optimal sequences of inhibitors bound at each of the three primary active sites. Furthermore, the assay can be performed in crude protein extracts under a variety of conditions.

We chose two tetra-peptide vinyl sulfone inhibitors based on data obtained from this library approach [12] (Table 1). Results from this screening process indicated that selection of a positively charged basic residue at the P3 position results in selectivity for the β2 subunit responsible for the trypsin-like activity of the proteasome. The library data also indicated that a proline or tyrosine residue at P4 further increases specificity for the β2 subunit. We therefore chose the peptide Ac-PRLN-VS (MB1) as our β2-selective inhibitor. This compound was previously shown to bind exclusively to the β2 subunit at concentrations as high as 100 μM, suggesting that it is unable to occupy the active sites of β1 and β5. The library results also indicated that simple replacement of the basic residue at P3 with an aliphatic leucine residue abolishes the selectivity of the inhibitor. We therefore chose the sequence Ac-YLLN-VS as a general inhibitor that differed from MB1 only in the P3 and P4 residues. This compound was shown to bind equally well to each of the three active sites. Assay of these inhibitors against purified 20S proteasomes indicated that MB1 inhibited hydrolysis of only the trypsin-like

substrate (Boc-LRR-MCA) while MB2 inhibited hydrolysis of the chymotrypsin-like (Suc-LLVY-MCA), trypsin-like, and PGPH (Ac-LLE-MCA) substrates (data not shown).

Structure of MB1 Bound to the β2 Subunit: Critical Binding Determinants at the P3/S3 Interface

To obtain the structures of the inhibitor-bound 20S proteasomes, crystals were soaked for 6 hr with the inhibitors. Determination of the three-dimensional structures of the complexes indicated that, as expected, MB1 was covalently bound to only the β2 active site while MB2 was bound to the active sites of β1, β2, and β5. The structure of the β2 active site containing the covalently bound MB1 ligand (Ac-PRLN-VS) shows the P3 arginine residue projected into a deep acidic pocket at the S3 subsite (Figure 2A). The P1 asparagine is likewise buried into a slightly less pronounced acidic S1 pocket. The large size and the acidic nature of the S3 pockets explains the reason for favorable selection of lysine and arginine residues at the P3 position of the previously identified β2-specific inhibitors [12]. In addition to the overall acidic nature of the S3 pocket, several residues within this site are available for hydrogen bonding interactions with the side chain nitrogen residues of arginine (Figure 2B). In particular, aspartic acid 28 of the β2 subunit and cysteine 118 of the adjacent β3 subunit project into the S3 pocket and make favorable hydrogen bond interactions with nitrogens of the P3 arginine. These interactions are likely to be one of the critical determinants for selectivity at the S3 site of the trypsin-like active site.
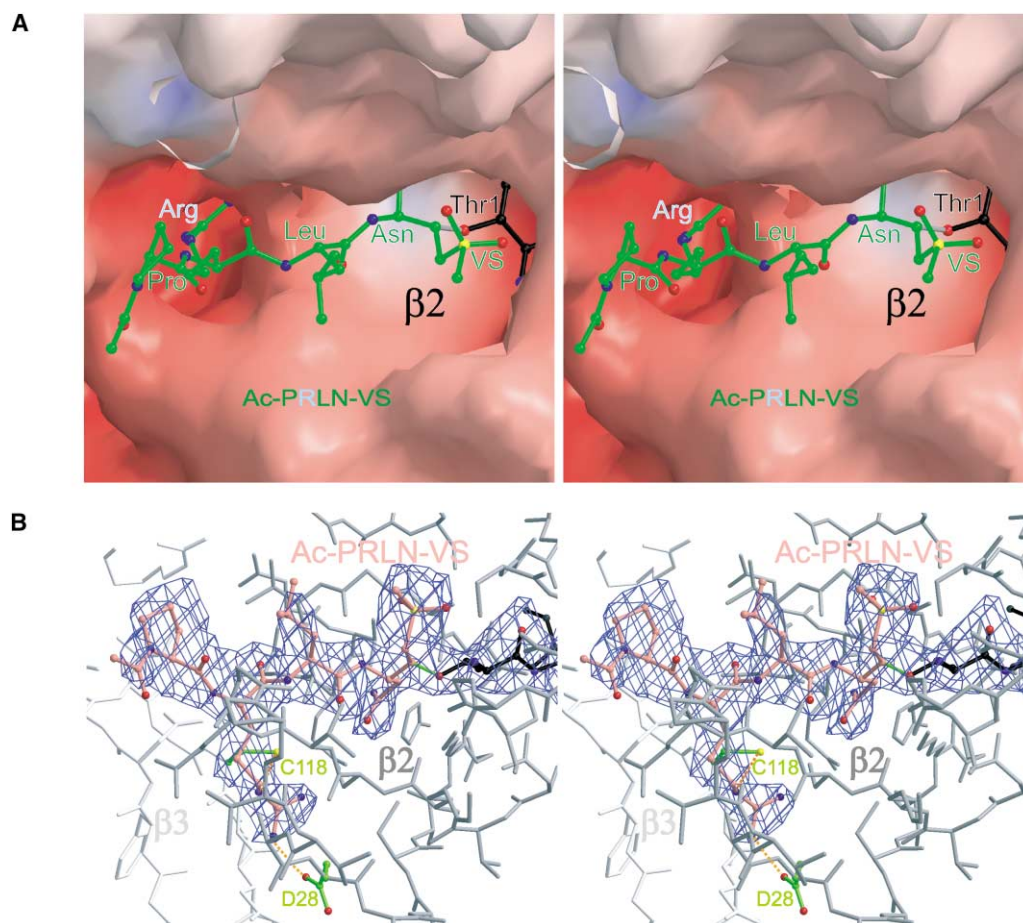
Figure 2. Structure of the β2-Specific Inhibitor MB1 Bound to the Trypsin-Like Active Site of the Yeast 20S Proteasome

(A) Surface model of MB1 bound in the trypsin-like active site with contacts to the β2 and β3 subunits. The catalytic N-terminal threonine is covalently linked to the inhibitor and is shown in black. Colors indicate positive and negative electrostatic potential contoured from 15kT/e (intense blue) to −15 kT/e (intense red).

(B) Wire frame structure of MB1 bound in the trypsin-like active site. Favorable hydrogen bonds between Asp28 of β2 at the bottom of the S3 pocket and Cys118 of β3 within the walls of the S3 pocket are shown. These residues make productive contacts with the amine groups of the P3 arginine of MB1.

The P2 and P4 residues of MB1 appear to play only a minor role in contributing to the binding interactions between the inhibitor and the β2 active site. The P2 residue, in particular, projects into the central core of the 20S cavity, making little or no contacts with the β2 subunit. The P4 proline residues forces a slight kink in the inhibitor backbone that causes the N-terminal portion of the inhibitor to bend away from the inner cavity wall and reduces the contacts between the inhibitor and the adjacent β3 subunit. Furthermore, the S4 pocket of β2 is quite small, thereby making the proline in P4 an ideal residue for binding to this subunit. This relatively small S4 pocket may also represent a means for creating inhibitors that can be excluded from binding to β2 through addition of bulky hydrophobic groups at the P4 position.
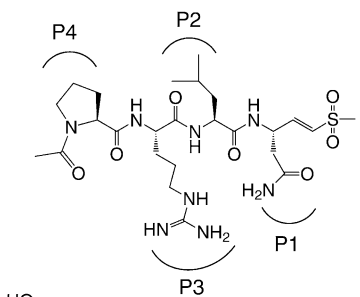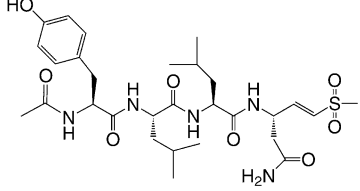
The vinyl sufone group forms a covalent bond with the hydroxyl residue of the N-terminal threonine. Strong binding interactions result from three hydrogen bonds between the sulfone oxygens and backbone amides as well as the free amino terminus of Thr1. These hydrogen bonds may help explain why the vinyl sulfones react covalently with the hydroxyl nucleophile of the proteasome even though these electrophiles were originally designed as mechanism-based inhibitors of cysteine proteases [24]. Such hydrogen bonding interactions may be important for activation of the electrophilic vinyl carbons as well as to retain the bound inhibitor in the active site, thereby increasing the likelihood of a covalent attack by the hydroxyl nucleophile.

Structure of MB2 Bound to the β1, β2, and β5 Subunits: Potential Conflicts at S3?

In addition to the favorable interactions of MB1 with the β2 active site, we wished to explore whether additional nonfavorable interactions exist that would exclude MB1 from binding to the β1 and β5 active sites. To explore the reasons for lack of binding at β1 and β5, we determined the structure of the core particle bound to the compound MB2. Figure 3 shows the surface structures of the inhibitor bound into each of the three primary active sites of the complex.

Table 1. Chemical Structures and Subunit Specificities of the Two Peptide Vinyl Sulfone Proteasome Inhibitors

Compound	Structure	Subunits Inhibited
MB1 Ac-PRLN-VS		β2 Only
MB2 Ac-YLLN-VS		β1, β2, β5

MB2 adopted a similar binding mode within all three active sites. Furthermore, its orientation was similar to that of MB1, binding such that the P1 and P3 residues made direct contacts with the cavity walls while the P2 and P4 residues projected in the opposite direction. However, several minor differences between the backbone structures of MB1 and MB2 were observed. The most noticeable difference was observed for the P4 tyrosine residue of MB2. This large phenolic ring was oriented so that it made favorable binding contacts with the adjacent subunits that make up the extended S4 pockets of each of the three active sites. In particular, the contacts between the P4 tyrosine and the S4 pocket of the β5/β6 chymotrypsin site seemed to be critical for favorable binding. This result is consistent with the finding that tetrapeptides that contain a hydrophobic P4 residue are potent inhibitors of the chymotrypsin-like activity but can be rendered completely inactive upon removal of the P4 residue [15]. Furthermore, addition of P4 residue to known tripeptide cysteine protease inhibitors can likewise result in increased cross-reactivity with the proteasome (unpublished data). These results are also consistent with the P3 and P4 positions on a substrate making the primary interactions with the β5/β6 interface that control the sequence specificity at this site.

In the case of all three primary active sites, the S3 pockets are large open spaces created at the interfaces between the primary catalytic subunits and the backsides of adjacent β subunits. Since these pockets are large, it seemed unlikely that they would be capable of excluding specific side chain residues, even large positively charged groups such as arginine. To confirm this, we superimposed the structure of the β2 bound MB1 onto that of MB2 bound to both β1 and β5 to determine if potential steric or electrostatic clashes existed that could further explain the high degree of selectivity of MB1 (data not shown). These structures indi-

cated that while the β1/β2 and β5/β6 S3 sites lacked the residues for hydrogen bond interactions with the P3 arginine of MB1, neither structure indicated sites of steric or electrostatic clashes. These findings suggest that simply losing favorable interactions at the S3-P3 interface are sufficient to prevent covalent modification at the catalytic nucleophile two residues away. While covalent inhibitors may not perfectly mimic a true protein substrate, these results suggest that interactions at the S3 site may drive selectivity by effectively holding a substrate in place long enough for hydrolysis to occur.

Analysis of the S1 pockets of each of the three active sites occupied by the asparagine of MB2 indicate that these relatively shallow pockets are able to accommodate an amide side chain regardless of the topology and electrostatic character observed for each active site. In the case of the β2 subunit, the S1 site contains an acidic pocket that would be expected to interact favorably with the P1 side chain amide of MB2. Likewise, the shallow S1 pocket of β5 contains a methionine residue that would be expected to tolerate the P1 asparagine residue. However, the basic character of the S1 binding site of β1 would be predicted to disfavor binding of the P1 residue of MB2. The fact that MB2 is able to be covalently bound to each of these active sites with relatively diverse S1 pockets suggests that this site may in fact be of secondary importance to interactions that take place at the S3 and S4 subsites. This model for binding is further supported by the finding that the overall electron density for MB2 bound in each of the three active sites is low, indicating relatively poor binding interactions overall. However, the fact that MB2 serves as a reasonably potent inhibitor and forms covalent interactions with each active site suggests that even with unfavorable P1 interactions, it may be possible for a peptide substrate to be hydrolyzed. In the case of MB1, strong favorable interactions at P3 in the β2/β3 trypsin site make up for the relatively poor P1 residue, leading to a highly selective inhibitor.
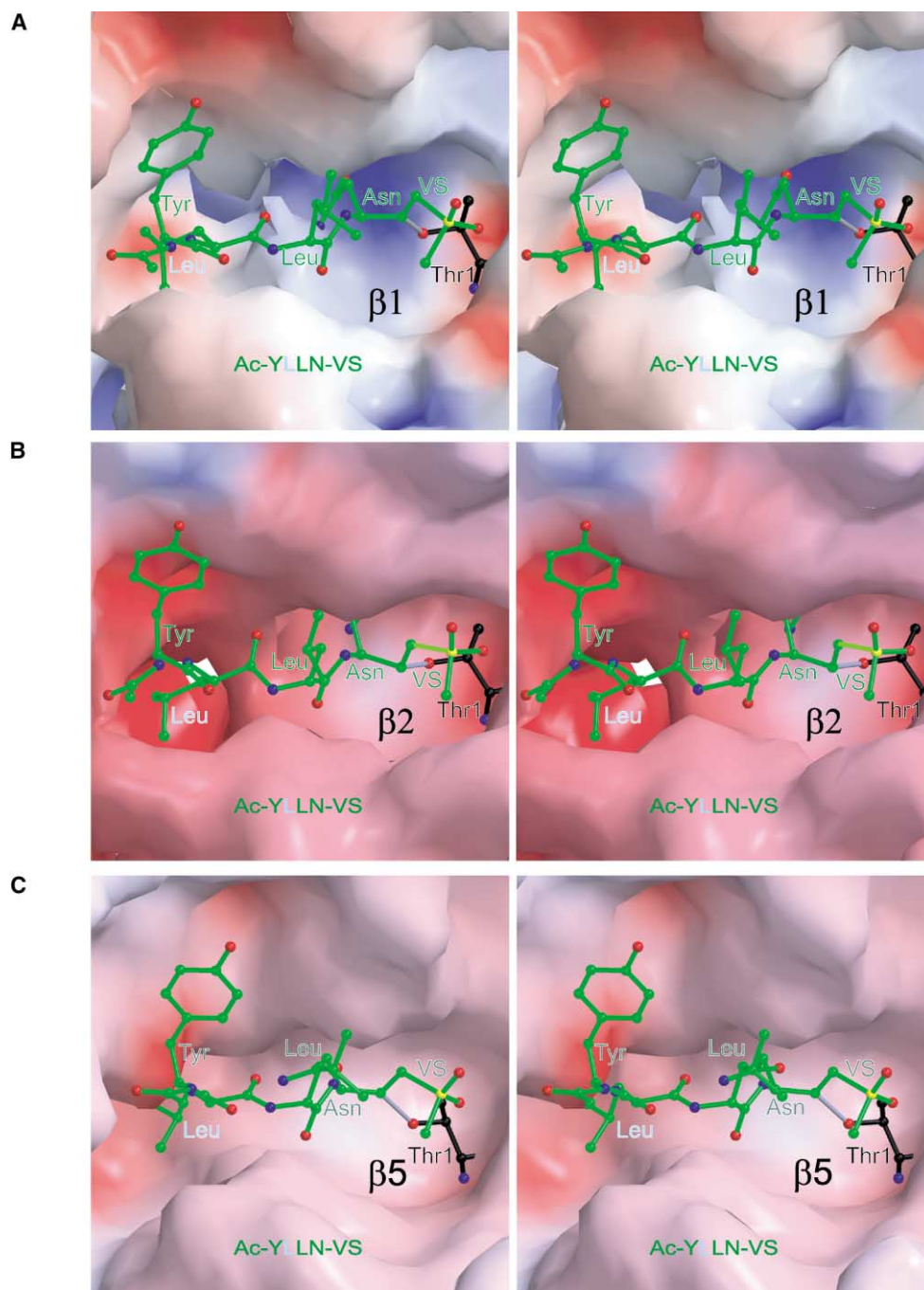
Figure 3. Structures of MB2 Bound into Each of the Three Primary Active Sites of the Proteasome

MB2 covalently bound into the PGPH active site (top panels), the trypsin-like site (middle panels), and the chymotrypsin-like site (bottom panels). The S3 site is found at the interface between each catalytic β subunit and its nearest neighbor subunit. Note the overall similarity in the binding mode of the inhibitor regardless of the net charge in the P1 pocket. In all cases, the S3 subsite is the largest pocket and is occupied by the critical P3 residue of the inhibitor. Colors indicate positive and negative electrostatic potential contoured from 15kT/e (intense blue) to −15 kT/e (intense red).

Overlay of MB1, MB2, Epoxomicin, and TMC-95A Backbone Structures: Implications for the Design of Subunit-Selective Noncovalent Inhibitors

The crystal structures of the natural products epoxomicin and TMC-95A (for chemical structures see Figure 4A) bound to the 20S proteasome have recently been reported [25, 26]. These structures can be used to compare the overall binding topology of multiple inhibitors within the active sites of the proteasome. Overlay of the structures of MB1, MB2, and epoxomicin bound to the 20S proteasome indicate a remarkable similarity in overall geometry (Figure 4B). In particular, the backbone
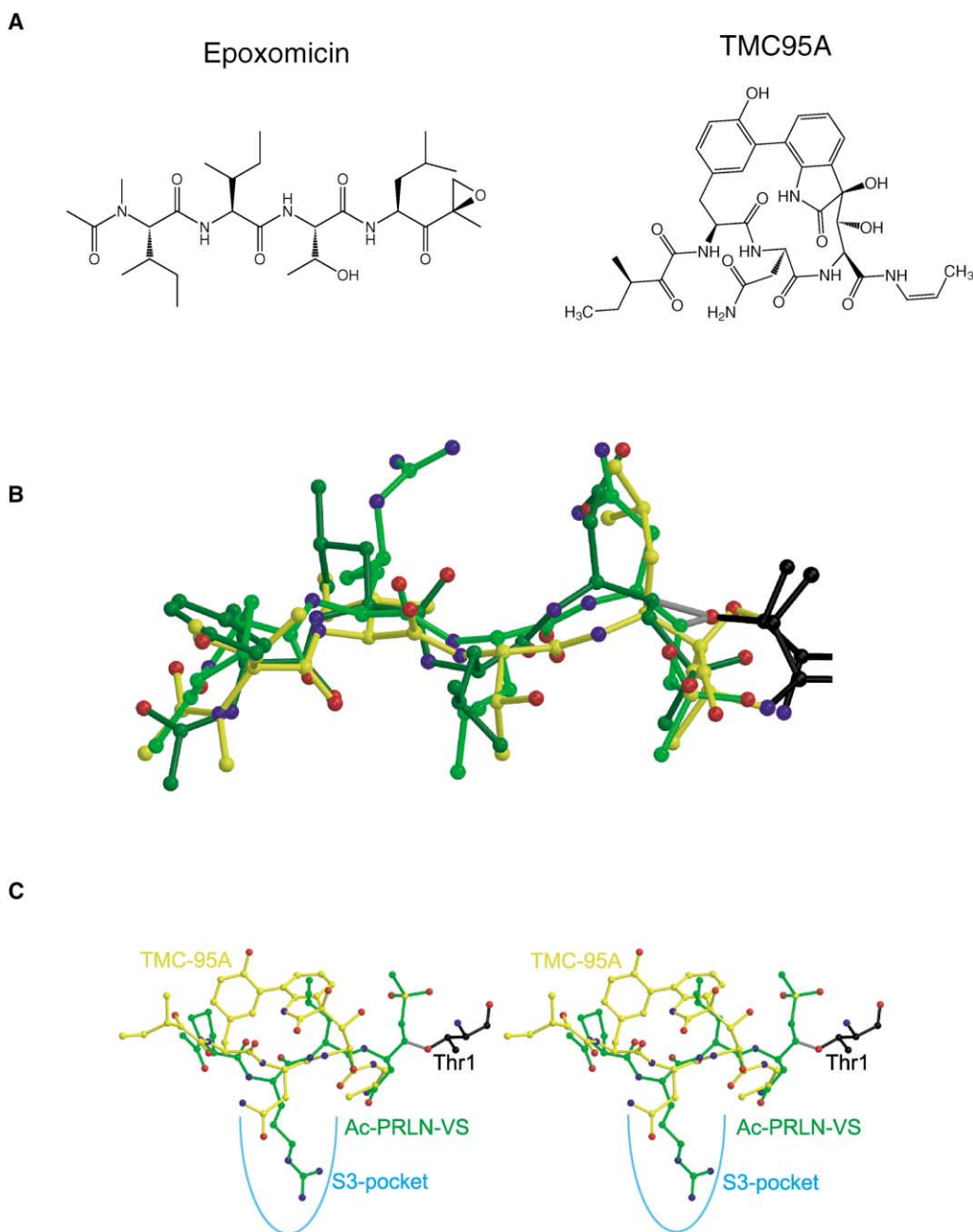
A

Epoxomicin

TMC95A

B

C

Figure 4. Comparison of Proteasome Bound MB1 and MB2 Structures with the Structures of the Natural Products Epoxomicin and TMC-95A

(A) Chemical structures of the natural products epoxomicin and TMC-95A.

(B) Superimposition of the coordinates of MB1 (light green), MB2 (dark green), and epoxomicin (yellow) bound to subunit β2. All three inhibitors have a similar peptide backbone but different side chain residues and electrophilic "warheads." Note the general binding mode for all three inhibitors within an active site of the proteasome.

(C) Overlay of bound structure of MB1 with TMC-95A. The overlay reveals the amide moiety of TMC-95A that mimics the P3 residue of the specificity determining arginine of MB1.

structures of all three bound inhibitors are nearly identical, suggesting that each compound is rigidly held in position such that its side chains are projected toward the binding pockets of the protein in a specific manner. This finding is particularly surprising considering the relatively dissimilar primary sequence and type of electrophiles found on epoxomicin when compared to MB1 and MB2 and suggests that inter-side chain interactions play little if any role in how the inhibitor is presented to the active site. It also indicates that changes in overall backbone structure resulting from a change from P3 leucine (MB2) to P3 arginine (MB1) are not responsible for the high degree of subunit selectivity of MB1.

The rigidity with which straight chain peptide-based

Table 2. Crystal Data

	YLLN-VS	PRLN-VS
Cell constants (Å)	a = 136.5; b = 302.0; c = 145.0; β = 112.6	a = 135.8; b = 301.1; c = 144.0; β = 112.8
Resolution (Å)	50–2.95	50–3.1
Observation, 2σ	1,150,929	436,438
Uniques	299,192	141,363
Completeness	98.0	90.5
R_{merge} %	8.4	13.9
R/R_{free} %	25.8/29.8	26.6/32.9
Rms bonds, Å	0.013	0.013
Rms angles, °	1.885	2.009

inhibitors bind to each of the multiple active sites prompted us to compare the bound structures of MB1 with that of the cyclic peptide natural product TMC-95A. This noncovalent small molecule shows strong binding to primarily the chymotrypsin-like site of the 20S proteasome. Analysis of the TMC-95A structure overlaid with that of MB1 shows remarkable overlap with both the backbone amides and the P1 asparagine and P3 arginine residues (Figure 4C). Since TMC-95 interacts with the proteasome in a reversible manner, it must be capable of presenting functional groups in such a way that covalent attachment to the catalytic nucleophile is no longer required. The exceptional potency of the TMC-95 analogs indicates that tight binding interactions at these two sites must be sufficient to lock the inhibitors in the active site and inhibit turnover of substrates.

Coupling information from the structures of MB1, MB2, and TMC-95A suggests that it should be possible to generate a scaffold based on the geometry of the bound TMC-95A that can present a variety of structures to the S1 and S3 pockets in each of the active sites of the proteasome. By modulating these structures with respect to the P3 position, it should be possible to fine-tune the selectivity of the compounds for individual β subunits. The results from the MB1 structure presented here support the fact that simple hydrogen bonding interactions at the S3-P3 interface can be sufficient to control this absolute specificity.

Significance

The proteasome is a large, multicatalytic protease complex responsible for breakdown of most cytosolic proteins [1]. While its three-dimensional structure and mechanism of hydrolysis have been determined, little is known about the elements that control the primary sequence specificity of the complex. Previous work using libraries of peptide-based covalent inhibitors has identified structural elements that can be used to control the substrate selectivity of synthetic inhibitors [12, 13]. We present here the structures of two covalent inhibitors, MB1 and MB2, that differ only in their P3 and P4 residues, bound to the core 20S proteasome particle. These structures suggest that favorable interactions between the P3 residue of MB1 and the large S3 pocket generated at the interface of the β2 and β3 subunits are responsible for driving inhibitor selectivity. Furthermore, the P1 asparagine of MB1 and MB2 was bound in the S1 pocket of each of the active sites, regardless of seemingly unfavorable electrostatic in-

teractions. Taken together, these results suggest a model in which specificity can be controlled predominantly by interactions at the S3 site for substrates with favorable interactions at this site and poor interactions at other sites. However, strong interactions at P1 may overcome the need for a favorable P3 residue. This model for substrate binding may aid in the development of inhibitors of the proteasome with tunable selectivity for each of the active sites. The proteasome-bound structures of MB1, MB2, and the natural products epoxomicin and TMC-95A indicate a highly conserved binding mode that could facilitate design of rigid scaffolds that display functional groups to the critical substrate binding pockets within each active site. Such compounds may be effective for disrupting protein breakdown in a controlled manner, thereby reducing the overall toxicity associated with complete inhibition of all three active sites.

Experimental Procedures

Selection and Synthesis of Covalent Inhibitors

Tetrapeptide vinyl sulfones MB1 and MB2 were selected based on positional scanning library data generated for the proteasome in crude cell homogenates [12]. Compounds were synthesized using a mixture of solution and solid phase chemistries as previously described [12]. Compounds were first tested for potency against the three primary activities of purified 20S proteasomes. The results of these preliminary screens are reported elsewhere [12].

Structure Determination

Crystals of 20S proteasome from *S. cerevisiae* were grown in hanging drops at 24°C as described previously [4] and incubated for 6 hr with the vinyl sulfone compounds. The protein concentration used for crystallization was 40 mg/ml in 10 mM Tris-HCl (pH 7.5) and 1 mM EDTA. The drops contained 3 μl protein and 2 μl of the reservoir solution containing 30 mM magnesium acetate, 100 mM morpholino-ethane-sulphonic acid (pH 7.2), and 10% MPD.

The space group of the crystals belongs to P2₁ (see Table 2). Data were collected using synchrotron radiation with λ=1.05 Å on the ID14-beamline at ESRF/Grenoble/France. Crystals were soaked in a cryoprotecting buffer (30% MPD, 20 mM magnesium acetate, 100 mM morpholino-ethane-sulfonic acid [pH 6.9]) for 30 s and frozen in a stream of liquid nitrogen gas at 90 K (Oxford Cryo Systems). X-ray intensities were evaluated by using the MOSFILM program package (version 6.1) and data reduction was performed with CCP4 [27]. The anisotropy of diffraction was corrected by an overall anisotropic temperature factor by comparing observed and calculated structure amplitudes using the program X-PLOR [28]. Electron density was averaged 10 times over the 2-fold noncrystallographic symmetry axis using the program package MAIN [29]. Conventional crystallographic rigid body, positional, and temperature factor refinements were carried out with X-PLOR using the yeast 20S proteasome structure [4] as a starting model. For model building, the

program FRODO was used [30]. Modeling experiments were performed using the coordinates of yeast 20S proteasome with MAIN.

Figure Preparation

Figures 2A and 3 were prepared with GRASP [31] and MOLSCRIPT [32], and Figure 2B was prepared with BOBSCRIPT [33]. In Figures 4A and 4B, the pdb files were superimposed using top3d and illustrated with MOLSCRIPT. All these figures were rendered using the program RASTER3D [34].

References

1. Coux, O., Tanaka, K., and Goldberg, A.L. (1996). Structure and functions of the 20S and 26S proteasomes. Annu. Rev. Biochem. *65*, 801–847.
2. Stock, D., Ditzel, L., Baumeister, W., Huber, R., and Lowe, J. (1995). Catalytic mechanism of the 20S proteasome of Thermoplasma acidophilum revealed by X-ray crystallography. Cold Spring Harb. Symp. Quant. Biol. *60*, 525–532.
3. Löwe, J., Stock, D., Jap, B., Zwickl, P., Baumeister, W., and Huber, R. (1995). Crystal structure of the 20S proteasome from the archaeon *T. Acidophilum* at 3.4 Å resolution. Science *268*, 533–539.
4. Groll, M., Ditzel, L., Löwe, J., Stock, D., Bochtler, M., Bartunik, H.D., and Huber, R. (1997). Structure of 20S proteasome from yeast at 2.4 Å resolution. Nature *386*, 463–471.
5. Orlowski, M., and Wilk, S. (1981). A multicatalytic protease complex from pituitary that forms enkephalin and enkephalin containing peptides. Biochem. Biophys. Res. Commun. *101*, 814–822.
6. Wilk, S., and Orlowski, M. (1983). Evidence that pituitary cation-sensitive neutral endopeptidase is a multicatalytic protease complex. J. Neurochem. *40*, 842–849.
7. Tanaka, K., Ii, K., Ichihara, A., Waxman, L., and Goldberg, A.L. (1986). A high molecular weight protease in the cytosol of rat liver. I. Purification, enzymological properties, and tissue distribution. J. Biol. Chem. *261*, 15197–15203.
8. Orlowski, M. (1990). The multicatalytic proteinase complex, a major extralysosomal proteolytic system. Biochemistry *29*, 10289–10297.
9. Emori, Y., Tsukahara, T., Kawasaki, H., Ishiura, S., Sugita, H., and Suzuki, K. (1991). Molecular cloning and functional analysis of three subunits of yeast proteasome. Mol. Cell. Biol. *11*, 344–353.
10. Nussbaum, A.K., Dick, T.P., Keilholz, W., Schirle, M., Stevanovic, S., Dietz, K., Heinemeyer, W., Groll, M., Wolf, D.H., Huber, R., et al. (1998). Cleavage motifs of the yeast 20S proteasome beta subunits deduced from digests of enolase 1. Proc. Natl. Acad. Sci. USA *95*, 12504–12509.
11. Dick, T.P., Nussbaum, A.K., Deeg, M., Heinemeyer, W., Groll, M., Schirle, M., Keilholz, W., Stevanovic, S., Wolf, D.H., Huber, R., et al. (1998). Contribution of proteasomal beta-subunits to the cleavage of peptide substrates analyzed with yeast mutants. J. Biol. Chem. *273*, 25637–25646.
12. Nazif, T., and Bogyo, M. (2001). Global analysis of proteasomal substrate specificity using positional-scanning libraries of covalent inhibitors. Proc. Natl. Acad. Sci. USA *98*, 2967–2972.
13. Elofsson, M., Splittgerber, U., Myung, J., Mohan, R., and Crews, C.M. (1999). Towards subunit-specific proteasome inhibitors: synthesis and evaluation of peptide alpha′,beta′-epoxyketones. Chem. Biol. *6*, 811–822.
14. Groll, M., Heinemeyer, W., Jager, S., Ullrich, T., Bochtler, M., Wolf, D.H., and Huber, R. (1999). The catalytic sites of 20S proteasomes and their role in subunit maturation: a mutational and crystallographic study. Proc. Natl. Acad. Sci. USA *96*, 10976–10983.
15. Bogyo, M., Shin, S., McMaster, J.S., and Ploegh, H. (1998). Substrate binding and sequence preference of the proteasome revealed by active-site-directed affinity probes. Chem. Biol. *5*, 307–320.
16. Loidl, G., Groll, M., Musiol, H.J., Ditzel, L., Huber, R., and Moroder, L. (1999). Bifunctional inhibitors of the trypsin-like activity of eukaryotic proteasomes. Chem. Biol. *6*, 197–204.
17. Harris, J.L., Alper, P.B., Li, J., Rechsteiner, M., and Backes, B.J. (2001). Substrate specificity of the human proteasome. Chem. Biol. *8*, 1131–1141.
18. Vinitsky, A., Cardozo, C., Sepp-Lorenzino, L., Michaud, C., and Orlowski, M. (1994). Inhibition of the proteolytic activity of the multicatalytic proteinase complex (proteasome) by substrate-related peptidyl aldehydes. J. Biol. Chem. *269*, 29860–29866.
19. Myung, J., Kim, K.B., Lindsten, K., Dantuma, N.P., and Crews, C.M. (2001). Lack of proteasome active site allostery as revealed by subunit-specific inhibitors. Mol. Cell *7*, 411–420.
20. Thornberry, N.A., Chapman, K.T., and Nicholson, D.W. (2000). Determination of caspase specificities using a peptide combinatorial library. Methods Enzymol. *322*, 100–110.
21. Smith, M.M., Shi, L., and Navre, M. (1995). Rapid identification of highly active and selective substrates for stromelysin and matrilysin using bacteriophage peptide display libraries. J. Biol. Chem. *270*, 6440–6449.
22. Matthews, D.J., and Wells, J.A. (1993). Substrate phage: selection of protease substrates by monovalent phage display. Science *260*, 1113–1117.
23. Harris, J.L., Backes, B.J., Leonetti, F., Mahrus, S., Ellman, J.A., and Craik, C.S. (2000). Rapid and general profiling of protease specificity by using combinatorial fluorogenic substrate libraries. Proc. Natl. Acad. Sci. USA *97*, 7754–7759.
24. Brömme, D., Klaus, J.L., Okamoto, K., Rasnick, D., and Palmer, J.T. (1996). Peptidyl vinyl sulfones: a new class of potent and selective cysteine protease inhibitors. Biochem. J. *315*, 85–89.
25. Groll, M., Kim, K.B., Kairies, N., Huber, R., and Crews, C.M. (2000). Crystal structure of epoxomicin: 20S proteasome reveals a molecular basis for selectivity of alpha′,beta′-epoxyketone proteasome inhibitors. J. Am. Chem. Soc. *122*, 1237–1238.
26. Groll, M., Koguchi, Y., Huber, R., and Kohno, J. (2001). Crystal structure of the 20 s proteasome:TMC-95a complex: a non-covalent proteasome inhibitor. J. Mol. Biol. *311*, 543–548.
27. Lesslie, A.G. (1994). Mosfilm User Guide, Mosfilm Version 5.2 (Cambridge, UK: MRC Laboratory of Molecular Biology).
28. Brunger, A. (1992). X-PLOR Version 3.1. A System for X-Ray Crystallography and NMR (New Haven, CT: Yale University Press).
29. Turk, D. (1992). Improvement of a programme for molecular graphics and manipulation of electron densities and its application for protein structure determination. PhD thesis, Technische Universitaet Muenchen, Munich, Germany.
30. Jones, T. (1978). A graphic model building and refinement system for macromolecules. J. Appl. Crystallogr. *11*, 268–272.
31. Nicholls, A., Bharadwaj, R., and Honig, B. (1993). GRASP - Graphical representation and analysis of surface-properties. Biophys. J. *64*, A166–A170.
32. Karaulis, P. (1991). Molscript - A program to produce both detailed and schematic plots of protein structures. J. Appl. Crystallogr. *24*, 946–950.
33. Esnouf, R.M. (1997). An extensively modified version of MolScript that includes greatly enhanced coloring capabilities. J. Mol. Graph. Model *15*, 132–4, 112–3.
34. Merritt, E., and Murphy, M. (1994). Raster3D Version-2.0 - A program for photorealistic molecular graphics. Acta Crystallogr. *50*, 869–873.